Heliyon 8 (2022) e12570

Contents lists available at ScienceDirect

Heliyon

journal homepage: www.cell.com/heliyon

Research article

Characterizing treatment resistance in muscle invasive bladder cancer using the chicken egg chorioallantoic membrane patient-derived xenograft model

Hugo Villanueva [a,b], Gabrielle A. Wells [b], Malachi T. Miller [b], Mariana Villanueva [a], Ravi Pathak [a], Patricia Castro [b,c], Michael M. Ittmann [b,c], Andrew G. Sikora [d,2], Seth P. Lerner [e,*,1]

[a] Department of Otolaryngology-Head and Neck Surgery, Baylor College of Medicine, Houston, TX, 77030, USA
[b] Advanced Technology Core Facilities, Baylor College of Medicine, Houston, TX, 77030, USA
[c] Department of Pathology and Immunology, Baylor College of Medicine, Houston, TX, 77030, USA
[d] Department of Head and Neck Surgery, MD Anderson Cancer Center, Houston, TX, 77030, USA
[e] Scott Department of Urology, Dan L. Duncan Cancer Center, Baylor College of Medicine, Houston, TX, 77030, USA

ARTICLE INFO

Keywords:
Bladder cancer
CAM
Proteomics
Genomics
Chemotherapy
Kinase inhibitor
PDX
Targeted therapy
EGFR
HER2
CDK4/6

ABSTRACT

Background: Non-metastatic muscle invasive urothelial bladder cancer (MIBC) has a poor prognosis and standard of care (SOC) includes neoadjuvant cisplatin-based chemotherapy (NAC) combined with cystectomy. Patients receiving NAC have at best <10% improvement in five-year overall survival compared to cystectomy alone. This major clinical problem underscores gaps in our understanding of resistance mechanisms and a need for reliable pre-clinical models. The chicken embryo chorioallantoic membrane (CAM) represents a rapid, scalable, and cost-effective alternative to immunocompromised mice for establishing patient-derived xenografts (PDX) *in vivo*. CAM-PDX leverages an easily accessible engraftment scaffold and vascular-rich, immunosuppressed environment for the engraftment of PDX tumors and subsequent functional studies.

Methods: We optimized engraftment conditions for primary MIBC tumors using the CAM-PDX model and tested concordance between cisplatin-based chemotherapy response of patients to matching PDX tumors using tumor growth coupled with immunohistochemistry markers of proliferation and apoptosis. We also tested select kinase inhibitor response on chemotherapy-resistant bladder cancers on the CAM-PDX using tumor growth measurements and immuno-detection of proliferation marker, Ki-67.

Results: Our results show primary, NAC-resistant, MIBC tumors grown on the CAM share histological characteristics along with cisplatin-based chemotherapy resistance observed in the clinic for matched parent human tumor specimens. Patient tumor specimens acquired after chemotherapy treatment (post-NAC) and exhibiting NAC resistance were engrafted successfully on the CAM and displayed decreased tumor growth size and proliferation in response to treatment with a dual EGFR and HER2 inhibitor, but had no significant response to either CDK4/6 or FGFR inhibition.

Conclusions: Our data suggests concordance between cisplatin-based chemotherapy resistance phenotypes in primary patient tumors and CAM-PDX models. Further, proteogenomic informed kinase inhibitor use on MIBC CAM-PDX models suggests a benefit from integration of rapid in vivo testing of novel therapeutics to inform more complex, pre-clinical mouse PDX experiments for more effective clinical trial design aimed at achieving optimal precision medicine for patients with limited treatment options.

1. Introduction

Muscle invasive urothelial bladder cancer (MIBC) is a high grade cancer of the urothelial lining that has a poor prognosis when locally advanced or node metastatic with 5-year survival probability of 30–40%. Standard of care treatment consists of neoadjuvant cisplatin-based chemotherapy (NAC) followed by cystectomy or chemoradiation therapy. Outcomes for patients presenting with MIBC have not improved in recent years, and standard of care neoadjuvant chemotherapy provides at best <10% improvement in a five-year overall survival over cystectomy

* Corresponding author.
E-mail address: slerner@bcm.edu (S.P. Lerner).
[1] Lead contact.
[2] Co-senior authors.

https://doi.org/10.1016/j.heliyon.2022.e12570
Received 24 September 2022; Received in revised form 20 November 2022; Accepted 15 December 2022

alone. Furthermore, patients with residual muscle invasive disease following NAC are at high risk to succumb to their disease. The recent approval of Nivolumab (anti-PD-1 checkpoint inhibition) for adjuvant therapy provides some hope for improvement in outcome (Bajorin et al., 2021), but the majority of MIBC patients do not respond to checkpoint inhibitors. This paucity of therapeutic advances is in part due to the lack of reliable pre-clinical models that accurately predict response to chemotherapy and/or investigational therapeutic small molecules.

The chick embryo chorioallantoic membrane (CAM) represents a highly versatile, scalable, and cost-efficient xenograft platform. Since its utility as a self-contained in vivo model for cancer research was realized (Murphy, 1913), the CAM has been leveraged extensively to generate numerous tumor models (DeBord et al., 2018). The vascular CAM supports and nourishes the developing embryo, and can likewise support patient-derived xenograft (PDX) tumors and cancer cell lines. In addition to robust vasculature, the CAM is easily accessible and is naturally immune deficient during the majority of chick embryonic development. These characteristics make it an ideal platform to grow cell lines or primary human tumor tissue until the adaptive immune system matures at approximately embryonic day 18 (E18) and rejects the xenograft. Cell and primary tumor xenografts on the CAM form three-dimensional, vascularized tumors, which maintain properties of cancer cells growing in vivo that are often lost in two-dimensional or simple three-dimensional tissue culture models (Ribatti, 2014). Examples of such properties include epithelial stromal interactions, tumor angiogenic properties, and complex three-dimensional cell-to-cell interactions. These features make the CAM xenograft models ideal and well suited for studying cancer cell processes such as growth, invasion, angiogenesis, and metastasis of human tumor cells into the developing chick embryo visceral organs in a relatively short period of time (Deryugina and Quigley, 2008a; b; Ribatti, 2014; Vantaku et al., 2019; Vantaku et al., 2020).

We have previously investigated bladder cancer cell growth and metabolic pathways using the CAM model (Vantaku et al., 2019, 2020), melanoma growth and survival (Lopez-Rivera et al., 2014), breast cancer (Arnold et al., 2020), and prostate cancer metastasis (San Martin et al., 2017). Successful engraftment and growth on the CAM is defined by several parameters including visible tumor growth by brightfield imaging, histological analyses of cancer cell morphological characteristics, proliferation and apoptotic indices via Ki-67 and cleaved caspase 3, and tumor specific markers if known.

For the current study, we collected and banked dozens of tumors from bladder cancer patients pre- and post-chemotherapy. Preliminary kinome pulldown profiling of collected MIBC specimens resistant to NAC has revealed three promising kinases that display overactive kinase-substrate relationships indicating over-active phosphorylation events. We hypothesized that one or more of these over-active kinases may be responsible for the chemo-resistant phenotype observed in patients and leverage the CAM model for the rapid testing of small molecule inhibitors against such kinases. We describe herein an *in vivo* method to engraft primary tumors from MIBC patients on the chicken egg CAM-PDX model to rapidly generate models suitable for pre-clinical therapeutic testing. Our results suggest that targeting the epidermal growth factor receptor family of kinases may provide a way to circumvent MIBC cisplatin-based chemotherapy resistance. These PDX tumors offer the opportunity to inform future pre-clinical and subsequent clinical trials in an effort to streamline personalized medicine for otherwise terminal disease patients.

2. Methods

2.1. Human patient sample acquisition

All patients signed an informed consent and human bladder cancer specimens were obtained under our Institutional Review Board (IRB) approved biobanking protocol (H-14435). Clinical and pathologic data are linked to pathologic specimens through our IRB approved protocol for our patient database Caisis (H- 22878) and de-identified patient demographics are reported in Table 1. All chicken egg experiments were conducted in accordance with the American Veterinary Medical Association with the approval of Baylor College of Medicine's institutional animal care and use committee (AN-7103). Tumor tissue for CAM experiments was transported in cold RPMI-1640 medium (Thermo-Fisher). Tumor specimens were either engrafted directly on the CAM on the same day acquired or were cryopreserved in freezing medium (RPMI-1640 supplemented with 50% FBS and 10% DMSO).

2.2. Housing fertilized eggs

Fertilized, specific pathogen free eggs (Charles River) were maintained at room temperature upon receipt to allow for acclimation for a total of 2 hours. Eggs were placed narrow side pointing down on a crate and set in a proper incubator (i.e. either cabinet or table-top incubator with a turning rack) at a constant temperature of 37.8 °C and humidity levels of 60% for seven days, ensuring the turning racks alternate positions once every hour.

2.3. Egg preparation

Eggs are removed from incubator after seven days and a candling lamp is applied to the eggs by placing them up against the light source as previously published (Villanueva and Sikora, 2022). Briefly, fertilized eggs are drilled into by creating a 2 × 2 cm opening on the shell in order to expose the inner shell membrane (ISM). The ISM is removed to unmask the CAM while providing enough surface area to place a 12 mm silicone ring on the exposed membrane. A piece of transparent tape is placed over the shell opening to cover the exposed area and the eggs are moved to a tabletop incubator without any rotation and with a constant temperature of 37.8 °C and humidity levels of approximately 60% for a minimum of 2 hours prior to engraftment of tumors.

2.4. Tumor mincing, inoculation, and drug treatment

Matrigel® (Corning Life Sciences) is thawed on ice for several hours prior to engraftment. Using our published technique, tumor fragments are manually minced until completely dissociated into a uniform homogenate (Villanueva and Sikora, 2022). Tumor homogenates are reconstituted with equal parts of PBS (supplemented with magnesium and calcium) and Matrigel® and engrafted on the CAM within the silicone ring. Four days after engraftment, tumors on the CAM are treated topically with saline and/or DMSO vehicle control, gemcitabine (Catalog# 1288463, Millipore Sigma) and cisplatin (Catalog# 232120, Millipore Sigma), Afatinib (Catalog# S1011, Selleck Chemicals), Abemaciclib (Catalog# S5716, Selleck Chemicals), or AZD4547 (Catalog# S2801, Selleck Chemicals). Eggs received a daily treatment regimen until day seven of the study.

2.5. Tumor fragment inoculation on CAM

Viably frozen bladder tumors are retrieved from the cryogenic chest freezer and quickly thawed using a 37 °C water bath. Thawed tumors are immediately removed from cryogenic vials and transferred to cold, sterile PBS supplemented with pen-strep for a quick rinse inside a biosafety cabinet. Freshly-resected tumors from the O.R. are transported to the lab and washed in cold, sterile PBS supplemented with pen-strep. Fresh or thawed tumors are cut into 2–3 mm fragments on ice to deter necrosis. The tumor fragments are dipped in Matrigel® and placed directly on top of the CAM and inside the silicone ring. Number of eggs used and successful engraftments of tumor fragments are summarized in Table 2.

Table 1. Patient demographic information. NAC: neoadjuvant chemotherapy, GemCis; gemcitabine plus cisplatin, NED: no evidence of disease, MVAC: methotrexate, vinblastine, doxorubicin, and cisplatin, 5-FU: fluorouracil, MMC: mitomycin C, NA: Not applicable, Pre Chemo: pre chemotherapy in locally advanced or metastatic setting, XRT: radiation therapy, Pembro: pembrolizumab, Fresh: tumor specimen engrafted directly from operating room, Cryo: tumor specimen engrafted from cryopreserved specimen, Minced: tumor specimen was engrafted as finely minced homogenate, Fragment: tumor specimen was engrafted as 2–3 mm fragment.

Sample ID	Gender	Age	Ethnicity	Histology	Therapy Agent	Pre or Post NAC	Disease Status	Experiment
BGB987445	Male	80	Not Hispanic or Latino	Urothelial	GemCIS	Pre NAC	Dead from disease	PDX Growth Optimization (Fresh-Minced)
BGB420711	Male	72	Not Hispanic or Latino	Urothelial	MVAC	Pre NAC	Alive NED	PDX Growth Optimization (Fresh-Minced)
BGB649851	Male	71	Not Hispanic or Latino	Urothelial	No NAC	NA	Alive NED	PDX Growth Optimization (Fresh-Minced)
BGB247270	Male	83	Not Hispanic or Latino	Urothelial w/85% Squamous	5-FU/MMC	Pre Chemo/ XRT	Alive with disease	PDX Growth Optimization (Fresh-Fragment)
BGB676371	Male	62	Hispanic or Latino	Urothelial	MVAC	Pre NAC	Alive NED	PDX Growth Optimization (Fresh-Fragment)
BGB691147	Female	59	Not Hispanic or Latino	Squamous	Unknown	Pre Chemo	Alive with disease	PDX Growth Optimization (Fresh-Fragment)
BGB687812	Male	78	Not Hispanic or Latino	Urothelial	No NAC	NA	Alive, disease status unknown	PDX Growth Optimization (Cryo-Fragment)
BGB864465	Male	48	Not Hispanic or Latino	Urothelial	GemCIS	Pre NAC	Alive NED	PDX Growth Optimization (Cryo-Fragment)
BGB248720	Male	79	Not Hispanic or Latino	Urothelial	No NAC	NA	Alive NED	PDX Growth Optimization (Cryo-Fragment)
BGB331255	Male	77	Hispanic or Latino	Urothelial	GemCIS	Pre NAC	Alive NED	PDX Growth Optimization (Cryo, Fresh-Fragment)
BGB490421	Male	92	Not Hispanic or Latino	Urothelial	Capecitabine	Post NAC	Alive with disease	Chemotherapy Test
BGB450466	Female	70	Not Hispanic or Latino	Urothelial	GemCIS	Pre NAC	Dead from disease	Chemotherapy Test
BGB680543	Male	61	Black or African American	Urothelial	GemCIS + Celecoxib + Pembro	Pre NAC	Alive NED	Chemotherapy Test
BGB448649	Male	72	Not Hispanic or Latino	Urothelial	Gemcitabine	Pre NAC	Alive with disease	Chemotherapy Test
BGB450544	Male	63	Not Hispanic or Latino	Urothelial	GemCIS	Pre NAC	Alive with disease	Chemotherapy Test
BGB510249	Female	67	Not Hispanic or Latino	Urothelial	GemCIS	Pre NAC	Dead from disease	Chemotherapy Test
BGB450466	Female	70	Not Hispanic or Latino	Urothelial	GemCIS	Post NAC	Dead from disease	Kinase Inhibitor
BGB352747	Male	82	Not Hispanic or Latino	Urothelial	GemCIS	Post NAC	Dead from disease	Kinase Inhibitor
BGB644697	Male	61	Not Hispanic or Latino	Urothelial	GemCIS	Pre NAC	Alive NED	Kinase Inhibitor
BGB581979	Male	72	Not Hispanic or Latino	Urothelial	Gemcitabine + Cisplatin + Pembro	Post NAC	Deceased with unknown cause	Kinase Inhibitor
BGB540726	Male	56	Not Hispanic or Latino	Urothelial	GemCIS	Post NAC	Dead from disease	Kinase Inhibitor
BGB352747	Male	82	Not Hispanic or Latino	Urothelial	GemCIS	Post NAC	Dead from disease	Kinase Inhibitor

2.6. Tumor imaging and growth assessment

Prior to PDX removal from the CAM, photographic images are taken at days four (i.e., beginning of treatment) and seven (end of treatment) post inoculation. Tumor size is calculated by measuring the percent surface area of growth inside of the 9 mm silicone ring using ImageJ (ImageJ, RRID: SCR_003070) software. To calculate effects from drug treatments on tumor size, the delta of percent surface area between days four and seven is calculated and reported as normalized tumor size.

Table 2. CAM-PDX take rates from fresh and cryopreserved tumors engrafted as fragments in PDX Growth Optimization experiments listed on Table 1.

	Cryo-Fragments	Fresh-Fragments
Unique patient samples engrafted	3	4
Number of eggs used	28	13
Number of PDX models generated	9	9
Take rate	32.14%	69.23%

2.7. Tissue processing and histology

PDX tissues are removed by surgically dissecting the tumor and surrounding CAM and rinsing with sterile PBS on a 6 cm Petri dish. The removed tumor is resected from the CAM and either cryogenically preserved in freezing medium (RPMI supplemented with 50% FBS and 10% DMSO) and/or fixed in 10% neutral buffered formalin. Fixed tumors are subsequently processed for embedding and sectioning. Paraffin-embedded blocks are cut into 3 μm sections and stained with hematoxylin and eosin for histological analysis.

2.8. Immunohistochemistry

Sections (3 μm) are deparaffinized and rehydrated into 1X PBS through Xylenes (Sigma) and a series of graded ethanols. To retrieve antigens, slides are heated in 1 mM Sodium Citrate buffer at a pH of 6.0 under pressurized conditions using a decloaker (Biocare Medical). To prevent non-specific binding, sections are treated with 60 ul of blocking solution (1.25% goat serum, 5% BSA (Sigma), 0.5% Tween 20, and 1X PBS) for 1 h at room temperature. Ki-67 (1:200, Agilent, GA62661-2, RRID: AB_2687921) and cleaved caspase 3 (1:800, Cell Signaling Technology, 9661S, RRID: AB_2341188) are diluted in blocking solution. Slides are incubated with primary antibodies at 4 °C overnight. Slides are washed in 1X PBS supplemented with 0.04% Tween 20 and incubated with Biotinylated Goat Anti-Mouse (Ki-67) and Anti-Rabbit (cleaved

Table 3. Tabular results from chemotherapy and small molecule inhibitor dose response studies.

	Cisplatin	Gemcitabine	Combo	Afatinib	Abemaciclib	AZD4547
Best-fit values						
β0	1.3	1.9	2	2	1.6	1.6
β1	−0.0043	−0.0033	−0.0062	2.6	−0.00094	2.2
X at 50%	295	587	329	−0.76	1745	−0.73
Std. Error						
β0	0.25	0.49	0.77	0.8	0.56	0.67
β1	0.00097	0.001	0.0021	4.7	0.0011	3.1
X at 50%	63	149	106	1.5	1690	1.2
95% CI (profile likelihood)						
β0	0.80 to 1.8	1.0 to 3.0	0.74 to 3.9	0.63 to 4.0	0.63 to 2.9	0.39 to 3.1
β1	−0.0066 to −0.0026	−0.0055 to −0.0014	−0.011 to −0.0029	−2.1 to 29	−0.0030 to 0.0013	−1.6 to 17
X at 50%	191 to 445	353 to 1092	145 to 569	??? to −0.037	612 to ???	??? to −0.044
Odds ratios						
β0	3.5	6.7	7.7	7.5	5.1	4.9
β1	1	1	0.99	14	1	8.8
95% CI (profile likelihood) for odds ratios						
β0	2.2 to 5.8	2.8 to 20	2.1 to 51	1.9 to 53	1.9 to 18	1.5 to 23
β1	0.99 to 1.0	0.99 to 1.0	0.99 to 1.0	0.13 to 2539493970211	1.0 to 1.0	0.20 to 17869430
Is slope significantly non-zero?						
|Z|	4.4	3.1	3	0.57	0.89	0.7
P value	<0.0001	0.0018	0.0027	0.5719	0.3732	0.4822
Deviation from zero?	Significant	Significant	Significant	NS	NS	NS
Likelihood ratio test						
Log-likelihood ratio (G squared)	49	26	19	0.72	0.75	0.9
P value	<0.0001	<0.0001	<0.0001	0.3967	0.3853	0.3438
Reject Null Hypothesis?	Yes	Yes	Yes	No	No	No
P value summary	****	****	****	ns	ns	ns
Area under the ROC curve						
Area	0.75	0.82	0.87	0.52	0.58	0.58
Std. Error	0.046	0.071	0.081	0.14	0.14	0.12
95% confidence interval	0.66 to 0.84	0.68 to 0.96	0.71 to 1.0	0.25 to 0.79	0.31 to 0.85	0.34 to 0.81
P value	<0.0001	0.0001	0.0012	0.9131	0.5338	0.6812
Goodness of Fit						
Tjur's R squared	0.33	0.44	0.61	0.019	0.028	0.023
Cox-Snell's R squared	0.31	0.38	0.51	0.031	0.025	0.038
Model deviance, G squared	134	44	18	13	29	17
Equation	log odds = 1.3–0.0043*X	log odds = 1.9–0.0033*X	log odds = 2.0–0.0062*X	log odds = 2.0 + 2.6*X	log odds = 1.6–0.00094*X	log odds = 1.6 + 2.2*X
Data summary						
Rows in table	135	54	27	23	30	23
Rows skipped (missing data)	0	0	0	0	0	0
Rows analyzed (#observations)	135	54	27	23	30	23
Number of 1	79	35	15	21	24	20
Number of 0	56	19	12	2	6	3
Number of parameter estimates	2	2	2	2	2	2
#observations/ #parameters	67.5	27	13.5	11.5	15	11.5
# of 1/#parameters	39.5	17.5	7.5	10.5	12	10
# of 0/#parameters	28	9.5	6	1	3	1.5

caspase 3) secondary antibodies (1:250, Life Technologies) for 1 h at room temperature. Slides are incubated for 30 min at room temperature with Avidin-Biotin Complex (ABC) reagent (Vector Laboratories) and washed with 1X PBS supplemented with 0.04% Tween 20. Slides are treated with DAB substrate kit (Vector Laboratories) for 1 min, washed with distilled water, and counterstained with CAT Hematoxylin (Biocare Medical). Slides are then dehydrated through a series of ethanols and Xylenes, and mounted using Permount Mounting Medium (Electron Microscopy Sciences).

2.9. Statistical analysis

Dose response curves were generated using simple logistic regression with a goodness of fit and Area Under the Curve metrics. Tabular results for dose response curves are reported in Table 3. Tumor size is calculated as described above and the normalized tumor growth size differences between vehicle and treated eggs are assessed using a non-parametric, Mann Whitney test (Prism, GraphPad Software). Ki-67 and cleaved caspase 3 were quantified by taking a minimum of three representative images for each parent or CAM-PDX sample and counting the total number of Ki-67 or CC3 expressing cells and dividing them by the total number of nuclei in each 400× field. Differences in proliferation or apoptosis were analyzed using an unpaired t-test with Welch's correction.

3. Results

3.1. Muscle invasive bladder cancer PDX growth optimization on the chicken embryo CAM

Our first objective was to optimize the engraftment procedure of patient-derived MIBC xenografts using the CAM assay. To achieve this, we used both biobanked and fresh tumor samples obtained at the time of a transurethral resection of a bladder tumor (TURBT) procedure. These tumors contain a complete patient history profile that allowed selection of tumors that met the criteria of pre-neoadjuvant chemotherapy sensitive or resistant and post-neoadjuvant chemotherapy resistant outcomes. Two different approaches were tested including fine mincing and fragment engraftment on the CAM. Tumor sources included cryopreserved tumors and specimens obtained directly from the operating room, both comprising a subset of the total tumors utilized throughout this study (see specimens used for PDX Growth Optimization in Table 1). In order to confirm that tumors successfully engrafted on the CAM, we isolated a small piece of the tumor after engraftment on the CAM for selected tumors (Figure 1A, B, C, D) and processed the specimens for histological review. Our results show that most primary tumors engrafted on the CAM as minced homogenates adopt a different morphological phenotype compared to the parent tumors (Figure 1F & H). However, tumors engrafted on the CAM as small, undisrupted fragments grow well and display a histology that is reminiscent of the original tumor (Figure 1E & G). To confirm the fidelity of PDX tumors on the CAM, we compared the histological properties of original parent tumors to CAM-PDXs engrafted as tumor fragments. We found concordance in all tumors that successfully engrafted from cryopreserved and fresh tumors obtained directly from the operating room (Figure 2A, B, C, D). The take rates for tumors engrafted from cryopreserved fragments was 32% (9 of 28) vs. 69% (9 of 13) for tumor fragments that were obtained fresh directly from the operating room (Table 2). To determine viability of tumors engrafted on CAM-PDX we assessed proliferation and apoptosis using Ki-67 and cleaved caspase 3 markers, respectively. Proliferation was maintained mostly in CAM-PDX tumors to their parental counterparts (Figure 2E, F, G, H), although Ki-67 expression was better retained in tumors engrafted from frozen specimens compared to fresh ones (Figure 2M and O). Apoptosis did not increase significantly in tumors successfully grown on CAMs, except for one model tested (Figure 2I, J, K, L, N, P).

3.2. Chemotherapy dose response test on CAM model

In order to establish the appropriate dose for chemotherapeutic agents and kinase inhibitors that were to be tested on the CAM assay,

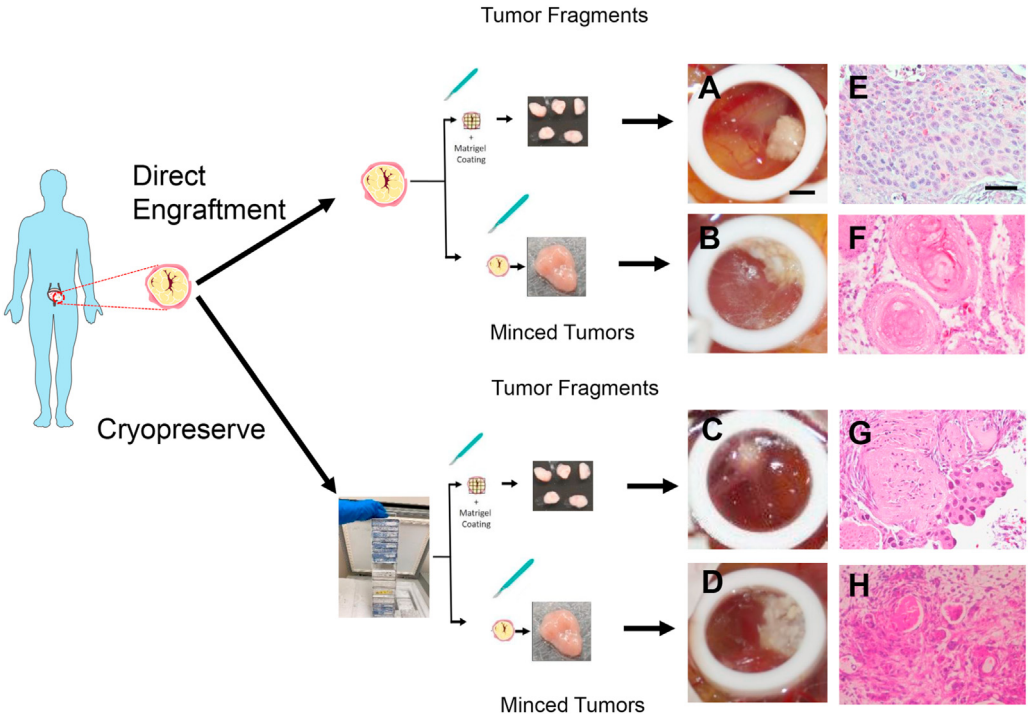

Figure 1. MIBC PDX growth optimization on CAM. Brightfield images of urothelial PDX on CAM from freshly obtained operating room tumors as A) fragments or B) minced products, cryopreserved tumors as C) fragments or D) minced products. Hematoxylin and eosin stained tumors from freshly obtained operating room tumors as E) fragments or F) minced products, and cryopreserved tumors as G) fragments or H) minced products. Scale bar = 2.25 mm (CAM tumors) and 50 μm (histology).

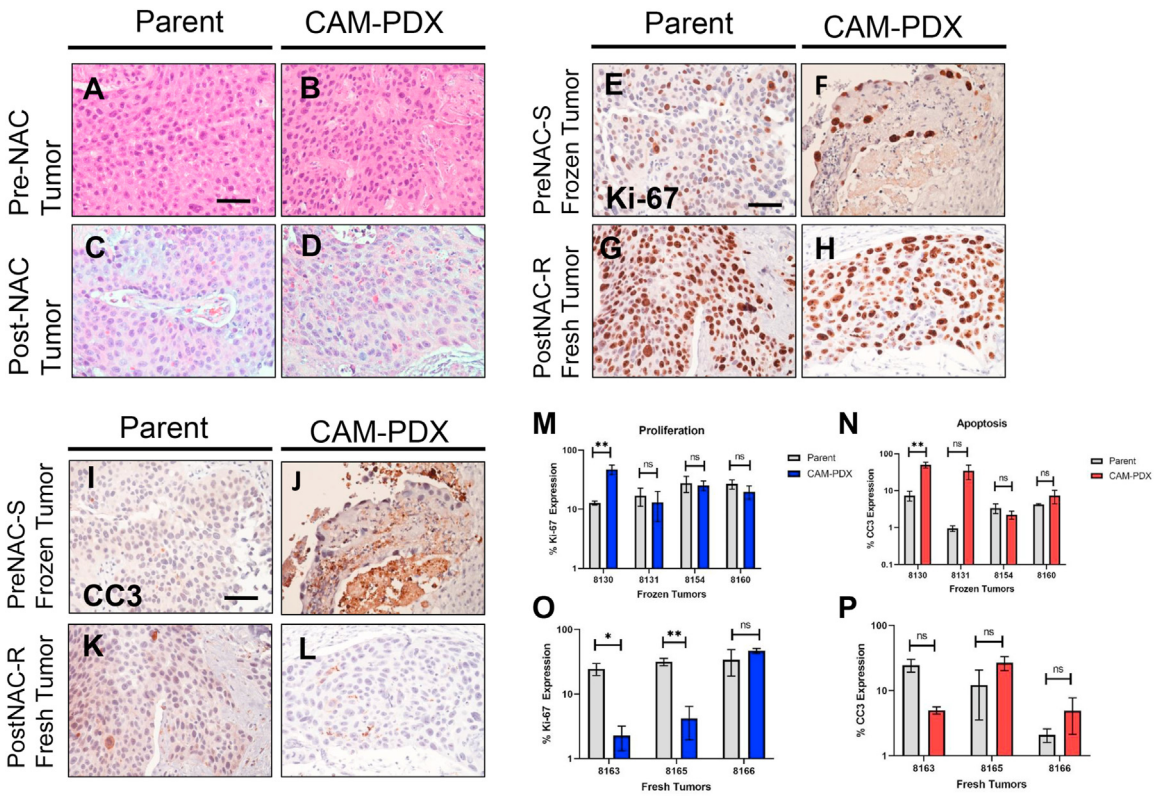

Figure 2. Histopathological concordance between parent and PDX tumors. Histology of urothelial cancer from patients prior to receiving neoadjuvant chemotherapy in A) Hematoxylin and eosin (H & E) parent tumors and B) matching CAM-PDX and tumor specimens after receiving neoadjuvant chemotherapy in C) hematoxylin and eosin parent tumor and D) matching CAM-PDX. Immunohistochemistry of pre-NAC cryopreserved for Ki-67 in E) parent tumors and F) CAM-PDX and cleaved caspase 3 in I) parent and J) CAM-PDX. Post-NAC freshly obtained tumor stained for Ki-67 in G) parent tumors and H) CAM-PDX and cleaved caspase 3 in K) parent tumors and L) CAM-PDX. Scale bar = 50 μm. Quantification of Ki-67 and CC3 in M-N) frozen and O–P) fresh tumors. *p < 0.05, **p < 0.01, ns: not significant. Data are represented as the mean ± S.E.M.

we performed a dose response curve on ungrafted, seven-day old chick embryos (E7) for a total of five days and assessed viability. To mimic the chemotherapeutic combination administered in the clinical setting, we treated embryos topically on ungrafted CAMs with cisplatin and gemcitabine independently and in combination at various concentrations (Figure 3). The LD50 for both cisplatin and gemcitabine when administered independently was 295 and 587 μM (Figure 3B and Table 3). Our results further demonstrated the LD50 for cisplatin and gemcitabine in combination was 329 μM, therefore, we reasoned that 50 μM of chemotherapy would be an acceptable dose that embryos with a tumor burden could tolerate. These results suggest that the CAM-PDX model can be used to test chemotherapy doses lower than 329 μM to interrogate the effects of cisplatin and gemcitabine on MIBC engrafted tumors.

3.3. Small molecule inhibitor dose response test on CAM model

We also tested the maximum tolerable dose of selected small molecule inhibitors on the CAM assay by performing subsequent dose response curves using the kinase inhibitors: Afatinib, Abemaciclib, and AZD4547. These small molecules target EGFR/HER2, CDK4/6, and FGFR respectively and were selected based on preliminary proteomics data (not shown) suggesting they are important in promoting growth of MIBC residual disease. Treatment at concentrations of each inhibitor up to 1 mM resulted in no significant lethality on chick embryos compared to the vehicle control group (LD50 > 1 mM). Results from these dose response curve studies suggest that EGFR/HER2, CDK4/6, and FGFR pathways are not critical for the viability of chick embryos at the doses and times given (Figure 4) and can therefore be safely used on the CAM-PDX model without compromising embryos.

3.4. Clinical resistance to cisplatin-based chemotherapy of pre-NAC MIBC tumors is maintained in CAM-PDX

To test concordance of parental tumor therapy response in the clinic with PDX tumors engrafted on the CAM, we performed a one-week chemotherapy treatment study on PDX tumors that were clinically defined as resistant to chemotherapy administered in the pre-neoadjuvant (pre-NAC) setting. Primary MIBC tumors were engrafted on the CAM and allowed to seed for three days and treated with a combination of cisplatin and gemcitabine chemotherapy daily for a total of four days. Treatment with chemotherapy failed to reduce gross tumor size (Figure 5A, B). Furthermore, treatment with chemotherapy increased Ki-67 and cleaved caspase 3 compared to vehicle treatment on CAM-PDX (Figure 5C). This result suggests that PDX tumors on the CAM recapitulate the clinical chemotherapy resistance phenotype of MIBC tumors treated in the neoadjuvant setting.

3.5. Chemotherapy resistant post-NAC MIBC PDXs respond to EGFR/Her2 inhibitor

After establishing a pre-NAC resistant model of MIBC on the CAM, we sought to demonstrate the feasibility of the CAM-PDX model by performing proof-of-concept studies using the selected kinase inhibitors tested in Figure 4. To perform these experiments, we employed primary MIBC tumors that were treated with chemotherapy and became resistant in the post neoadjuvant (post-NAC) setting (Table 1). Following seeding on the CAM, PDX tumors were allowed to engraft for three days and were treated with either Afatinib, Abemaciclib, or AZD4547 on day four. Tumors were measured at the time of initial treatment administration and at the end of the study. Tumor growth measurements show that Afatinib

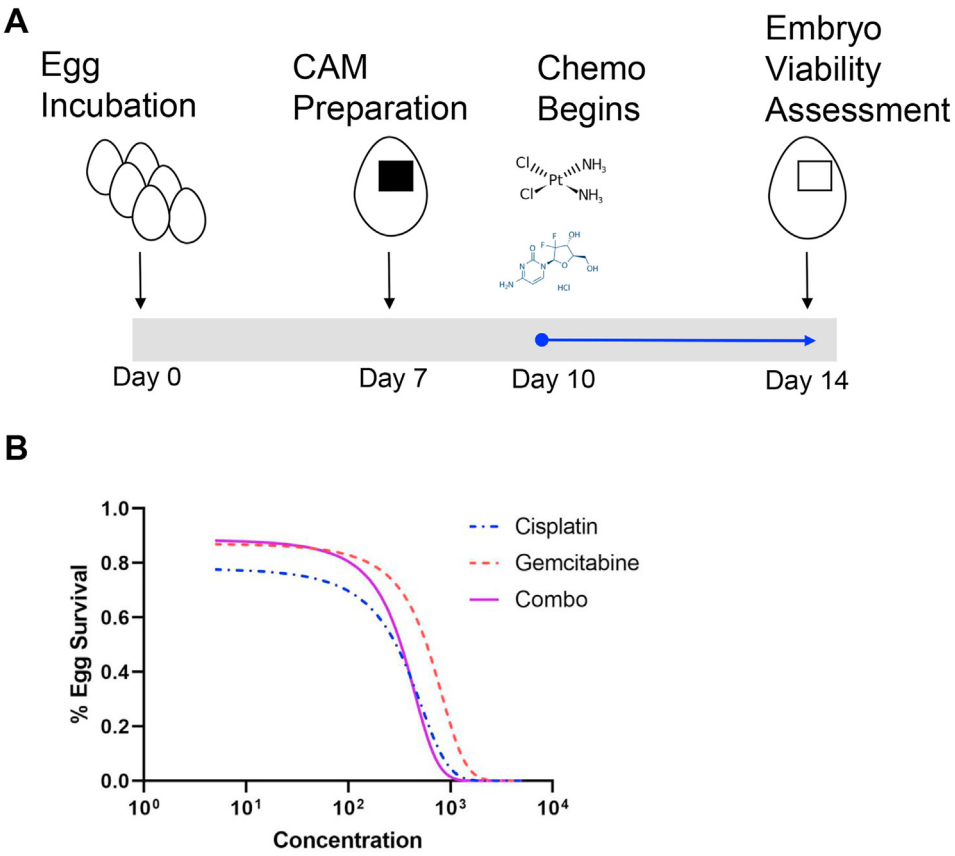

Figure 3. Effect of chemotherapy on chicken embryo viability. A) Schematic of chemotherapy dose response treatment on ungrafted chicken egg CAM. B) Cisplatin and gemcitabine independent treatment and combination dose response curves. Data are presented as an average of two to four independent experiments.

was the only inhibitor that reduced the size of tumors when compared to the vehicle control (Figure 6). In fact, Abemaciclib appears to promote tumor growth compared to the vehicle control, while AZD4547 has no obvious effect on gross tumors. These results suggest that EGFR/Her2 may be important for the growth of chemotherapy resistant bladder cancers.

4. Discussion

The CAM-PDX is continuously growing as an advanced 3D, *in ovo* model to leverage fertilized chicken embryo eggs for the engraftment of patient-derived tumor specimens. The results reported here are an extension of the ability of this assay to model patient urologic cancers (Hu et al., 2019; Vantaku et al., 2019). We report the optimization of growth conditions for MIBC tumors on the chicken embryo CAM for the purpose of testing novel compounds targeting chemotherapy-resistant bladder cancers. In addition, the CAM-PDX model is able to preserve the histological architecture, cell proliferation, and apoptotic phenotypes of matched parental tumors. Our cell proliferation data in matched parent tumors and xenografts engrafted from cryopreserved specimens (Figure 2M) versus freshly-obtained tumors (Figure 2O) was surprising given that we observe the opposite effect in breast cancer PDXs grown on CAM models. This discrepancy may be due to the small number of bladder cancer CAM-PDXs we have compared in our study and will likely improve as we increase our sample size. Furthermore, CAM-PDX model experiments demonstrate concordance with clinical outcomes of tumors in patients that received cisplatin-based chemotherapy and proof of principle studies support the feasibility of using this platform as a way to test small molecule inhibitors.

The availability of faster, cheaper, and feasible models without compromising fidelity of disease modeling is critical in the pre-clinical phase of therapeutic development. Our study reported here presents a method of employing the three R's in animal research (reduce, replace, and refine) as a strategy to quickly screen through promising, investigational compounds on patient-derived bladder tumors that have failed to respond to chemotherapy. Results from the current study demonstrate that the CAM-PDX model provides a niche for mimicking growth characteristics of the parental human tumors. The quick turnaround of this model allows investigators to test *in ovo* PDX tumor response to chemotherapy and small molecule inhibitors within a week of engraftment. Such expedited pre-clinical studies are invaluable towards informing more sophisticated and costly mouse PDX studies or can potentially be informative for clinicians treating patients presenting with locally advanced or metastatic bladder cancers.

The unique ability to employ the CAM platform for modelling of clinically-defined chemotherapy resistant bladder cancers is an invaluable tool that presents the opportunity for studying resistance mechanisms. The CAM-PDX assay as a true *in vivo* model recapitulates aspects of cancer not found in *in vitro* 3D models such as spheroids (e.g. vascularization), and engrafted tumors are far more accessible and amenable to manipulation than mouse PDX models. It also has the advantage of preserving the human tumor microenvironment with little interference from the chicken egg CAM stroma. While the CAM model has clear advantages, it also has limitations including current incapability of establishing stable PDX lines, inability to perform immuno-oncology studies, topical drug delivery methods may not be physiologically relevant, and a limited number of reagents (i.e. antibodies, primers, probes, etc.) that are compatible with avian species (DeBord et al., 2018; Ribatti, 2016). Of relevance to this study is the drug delivery via topical application of chemotherapy and small molecules, while very localized, has the possibility of not reaching the entire tumor area. This limitation requires further investigation by comparing topical versus injected compounds on

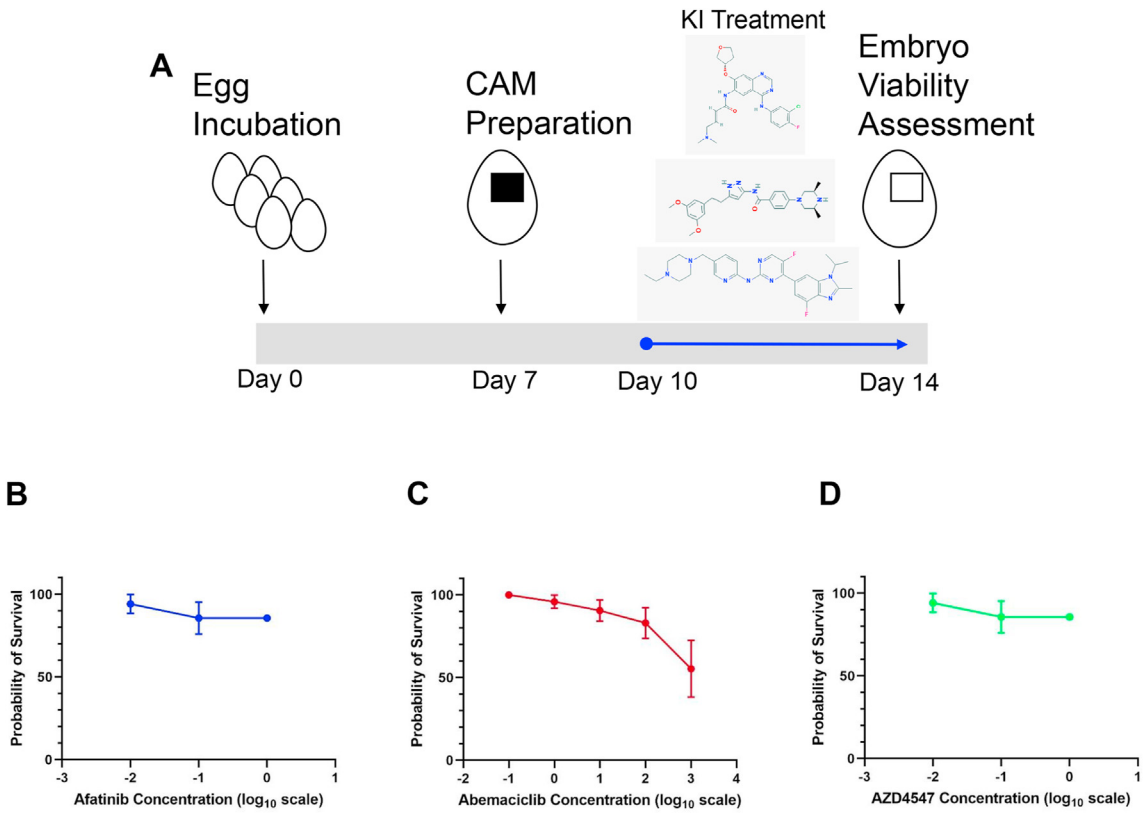

Figure 4. Effect of kinase inhibitors on chicken embryo viability. A) Schematic of kinase inhibitor dose response treatment on ungrafted chicken egg CAM. Kinase inhibitor dose response curves for B) Afatinib, C) Abemaciclib, and D) AZD4547. Data are represented as a percentage ±S.E.M.

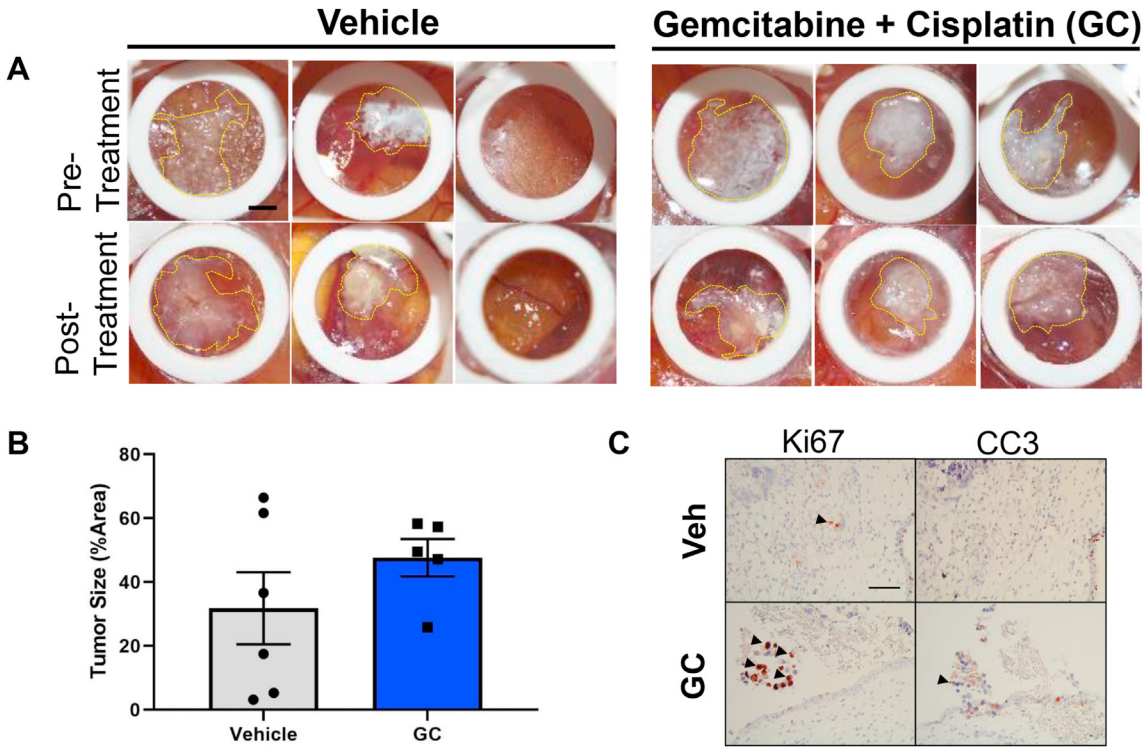

Figure 5. CAM-PDX chemotherapy resistance is concordant with that of pre-NAC MIBC tumors clinically resistant to GC. Brightfield photographs of MIBC chemo-resistant tumors engrafted on the CAM and treated with gemcitabine plus cisplatin (GC). B) Tumor size differences between vehicle and GC treated samples indicate a similar response to chemotherapy as their matched patient samples (patient tumor data not shown). C) Immunohistochemistry for proliferation marker Ki-67 and apoptosis marker cleaved caspase 3 in vehicle and GC chemotherapy. Arrowheads indicate positive staining. Scale bar = 2.25 mm (CAM tumors) and 50 μm (histology). Data are represented as the mean ± S.E.M.

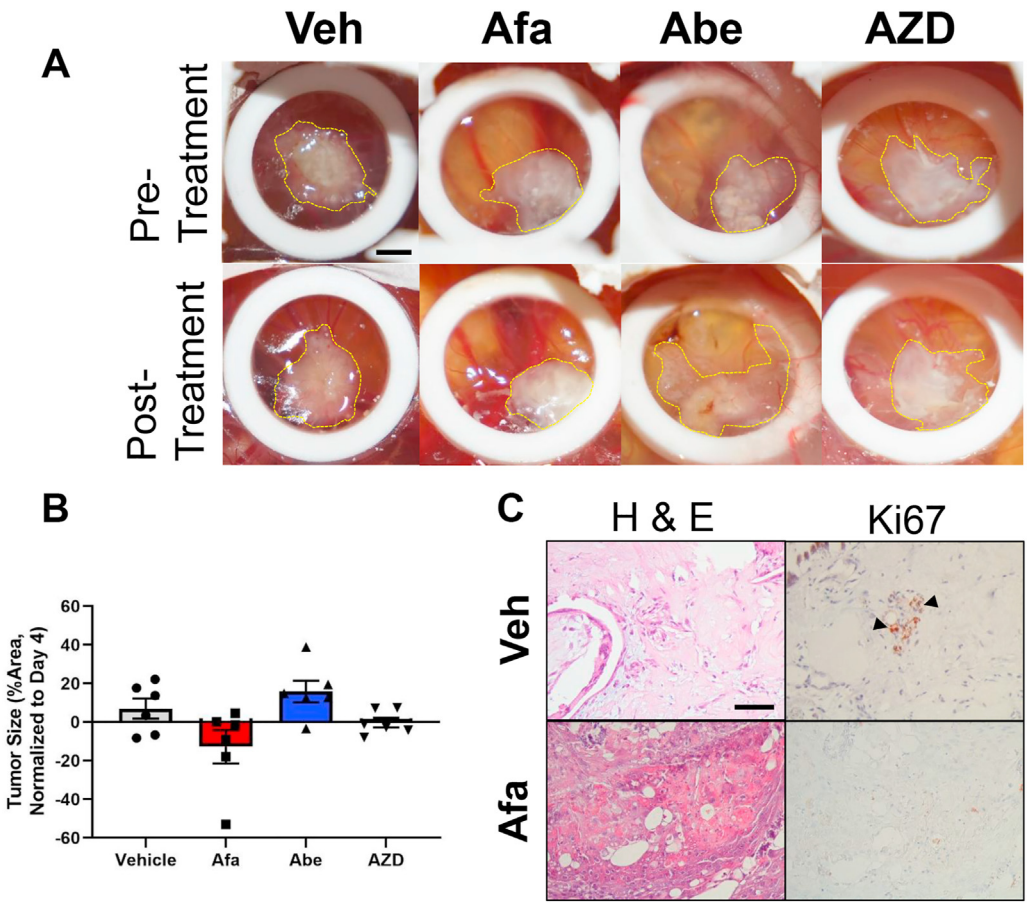

Figure 6. CAM-PDX kinase inhibitor response in post-NAC MIBCs clinically resistant to GC. A) Chemo-resistant tumors (post-NAC) engrafted on the CAM and treated with vehicle (Veh), afatinib (Afa), abemaciclib (Abe), and AZD4547 (AZD). B) Tumor size differences between vehicle and kinase inhibitor treated samples. Tumor growth is normalized to first day of treatment (i.e. day 4 post engraftment). Each data point represents a biological replicate. C) H & E and Ki-67 staining of vehicle and afatinib treated tumors. Arrowheads indicate positive stain. Scale bars = 2.25 mm (CAM tumors) and 50 μm (histology). Data are represented as the mean ± S.E.M.

the CAM and tracking their bioavailability and distribution via follow up studies with NMR spectroscopy or similar methods. These drawbacks are well known, however, the CAM model offers scalability coupled with low-cost, and is not subject to ethical restrictions that require prior approval notorious in rodent PDX models. As such, CAM-PDX models of bladder cancer offer unique and complimentary experiments to rodent PDX models that will save time and resources.

We present a compelling approach to model bladder cancers resistant to cisplatin-based chemotherapy. Our initial characterization efforts, while important for disease modeling, are only part of a larger effort to establish concurrence with human tumors. It will be equally important to employ next-generation sequencing technologies on CAM-based bladder cancer models in order to determine germline mutational status, copy number variations, transcriptomic, and proteomic profiling. Additionally, the CAM-PDX model versatility offers the ability to study other processes important to the development and progression of tumors (i.e. angiogenesis, invasion, metastasis, hypoxia, etc.) as well as the feasibility of employing longitudinal imaging and biosafety evaluation of promising compounds (Power et al., 2022; Sarogni et al., 2022). Such analyses will allow the assessment of tumor heterogeneity preservation and function on CAM-based models and better define their relevance to pre-clinical drug testing studies.

Declarations

Author contribution statement

Hugo Villanueva: Conceived and designed the experiments; Performed the experiments; Analyzed and interpreted the data; Wrote the paper.

Gabrielle A. Wells: Performed the experiments; Analyzed and interpreted the data; Wrote the paper.

Malachi T. Miller; Mariana Villanueva: Performed the experiments.

Ravi Pathak: Performed the experiments; Wrote the paper.

Patricia Castro; Michael M. Ittmann: Contributed reagents, materials, analysis tools or data; Wrote the paper.

Andrew G. Sikora: Conceived and designed the experiments; Wrote the paper.

Seth P. Lerner: Conceived and designed the experiments; Analyzed and interpreted the data; Wrote the paper.

Funding statement

This work was supported by the Bladder Cancer Advocacy Network and the U.S. National Cancer Institute (Cancer Center Support Grant #2P30CA125123).

Data availability statement

Data included in article/supp. material/referenced in article.

Declaration of interest's statement

The authors declare the following conflict of interests: AS reports Consultant: F. Hoffman La-Roche Pharma

SPL reports Clinical trials - Endo, FKD, JBL (SWOG), Genentech (SWOG), QED Therapeutics UroGen, Vaxiion, Viventia; Consultant/Advisory Board – Aura Bioscience, BMS, C2iGenomics, Ferring, Incyte, Pfizer/EMD, Protara, Stimit, Vaxiion, Verity Patent – TCGA classifier; Honoraria – Grand Rounds Urology, UroToday.

Additional information

No additional information is available for this paper.

Acknowledgements

Karoline Kremers and Dr. Kyle Drinnon for invaluable project management. The Patient-Derived Xenograft-Advanced In Vivo Models and Human Tissue Acquisition and Pathology Shared Resource Laboratories at Baylor College of Medicine for specimen collection and experimental protocols support.

References

Arnold, J.M., Gu, F., Ambati, C.R., Rasaily, U., Ramirez-Pena, E., Joseph, R., Manikkam, M., San Martin, R., Charles, C., Pan, Y., et al., 2020. UDP-glucose 6-dehydrogenase regulates hyaluronic acid production and promotes breast cancer progression. Oncogene 39, 3089–3101.

Bajorin, D.F., Witjes, J.A., Gschwend, J.E., Schenker, M., Valderrama, B.P., Tomita, Y., Bamias, A., Lebret, T., Shariat, S.F., Park, S.H., et al., 2021. Adjuvant Nivolumab versus placebo in muscle-invasive urothelial carcinoma. N. Engl. J. Med. 384, 2102–2114.

DeBord, L.C., Pathak, R.R., Villaneuva, M., Liu, H.C., Harrington, D.A., Yu, W., Lewis, M.T., Sikora, A.G., 2018. The chick chorioallantoic membrane (CAM) as a versatile patient-derived xenograft (PDX) platform for precision medicine and preclinical research. Am. J. Cancer Res 8, 1642–1660.

Deryugina, E.I., Quigley, J.P., 2008a. Chapter 2. Chick embryo chorioallantoic membrane models to quantify angiogenesis induced by inflammatory and tumor cells or purified effector molecules. Methods Enzymol. 444, 21–41.

Deryugina, E.I., Quigley, J.P., 2008b. Chick embryo chorioallantoic membrane model systems to study and visualize human tumor cell metastasis. Histochem. Cell Biol. 130, 1119–1130.

Hu, J., Ishihara, M., Chin, A.I., Wu, L., 2019. Establishment of xenografts of urological cancers on chicken chorioallantoic membrane (CAM) to study metastasis. Precis Clin Med 2, 140–151.

Lopez-Rivera, E., Jayaraman, P., Parikh, F., Davies, M.A., Ekmekcioglu, S., Izadmehr, S., Milton, D.R., Chipuk, J.E., Grimm, E.A., Estrada, Y., et al., 2014. Inducible nitric oxide synthase drives mTOR pathway activation and proliferation of human melanoma by reversible nitrosylation of TSC2. Cancer Res. 74, 1067–1078.

Murphy, J.B., 1913. Transplantability of tissues to the embryo of foreign species : its bearing on questions of tissue specificity and tumor immunity. J. Exp. Med. 17, 482–493.

Power, E.A., Fernandez-Torres, J., Zhang, L., Yaun, R., Lucien, F., Daniels, D.J., 2022. Chorioallantoic membrane (CAM) assay to study treatment effects in diffuse intrinsic pontine glioma. PLoS One 17, e0263822.

Ribatti, D., 2014. The chick embryo chorioallantoic membrane as a model for tumor biology. Exp. Cell Res. 328, 314–324.

Ribatti, D., 2016. The chick embryo chorioallantoic membrane (CAM). A multifaceted experimental model. Mech. Dev. 141, 70–77.

San Martin, R., Pathak, R., Jain, A., Jung, S.Y., Hilsenbeck, S.G., Pina-Barba, M.C., Sikora, A.G., Pienta, K.J., Rowley, D.R., 2017. Tenascin-C and integrin alpha9 mediate interactions of prostate cancer with the bone microenvironment. Cancer Res. 77, 5977–5988.

Sarogni, P., Mapanao, A.K., Gonnelli, A., Ermini, M.L., Marchetti, S., Kusmic, C., Paiar, F., Voliani, V., 2022. Chorioallantoic membrane tumor models highlight the effects of cisplatin compounds in oral carcinoma treatment. iScience 25, 103980.

Vantaku, V., Dong, J., Ambati, C.R., Perera, D., Donepudi, S.R., Amara, C.S., Putluri, V., Ravi, S.S., Robertson, M.J., Piyarathna, D.W.B., et al., 2019. Multi-omics integration analysis robustly predicts high-grade patient survival and identifies CPT1B effect on fatty acid metabolism in bladder cancer. Clin. Cancer Res. 25, 3689–3701.

Vantaku, V., Putluri, V., Bader, D.A., Maity, S., Ma, J., Arnold, J.M., Rajapakshe, K., Donepudi, S.R., von Rundstedt, F.C., Devarakonda, V., et al., 2020. Epigenetic loss of AOX1 expression via EZH2 leads to metabolic deregulations and promotes bladder cancer progression. Oncogene 39, 6265–6285.

Villanueva, H., Sikora, A.G., 2022. The chicken embryo chorioallantoic membrane (CAM): a versatile tool for the study of patient-derived xenografts. Methods Mol. Biol. 2471, 209–220.